Influence of source separation and montage on ictal source localization

L. Koessler, R. Salido-Ruiz, R. Ranta, V. Louis-Dorr, M. Gavaret, L. Maillard

***Abstract*— The aim of this paper is to evaluate the influence of the reference electrode (introduced to form an augmented average montage) and of the artifact elimination by blind source separation on the ictal electrical source imaging. We present here a preliminary study on one patient only. The results seem to indicate that the montage (and thus the reference handling method) has a limited but existent influence on the quality of the source localization. Artifact elimination highly improves this quality as well.**

I. Introduction

In the last decade different source models have been developed to estimate the localization of the intracerebral sources of the epileptic activity recorded by high resolution (HR) EEG. Equivalent current dipole (ECD) models are very often used to represent epileptic activity. Dipolar models can be characterized by three spatial coordinates (x, y, z) and three components (magnitude, moment, direction) which have to be estimated by EEG dipole analysis [1]. It has been shown that the EEG dipole source analysis is a useful tool in the presurgical evaluation in ictal EEG [2] as well as inter-ictal EEG [3, 4].

The most important drawbacks in ictal source localization are muscle activity and eye blink artifacts which represent two contributors to the distortions of the ictal surface EEG. During most epileptic seizure, muscle activity is very prominent and is reflected in the EEG by a high frequency random signal. Localizing the source during a temporal window of analysis with muscle activity will most likely result in a source close to the muscles. Usually a narrow bandpass filters around the frequency of the ictal discharge is use to remove the muscle and movement artifacts to obtain a signal with high signal-to-noise ratio [2]. However, the ictal EEG activity has a frequency of 0.5 between 45 Hz. Hence, the application of narrow band filters will filter out valuable information from the EEG [5].

Eye movements and blinks are other sources of non-cerebral activity which can distort the EEG. These artifacts are mainly recorded by the fronto-polar electrodes placed near the eyes. The characteristics are low frequency content, non-stationarity and high amplitude [6]. Blind Source Separation (BSS) techniques have shown promising artifact removal results [7, 8].

As said previously, localization is based on the scalp EEG. The raw EEG is a set of measured potentials with respect to a common reference, most often placed on head. This montage is commonly designated as the Common Reference Montage (CRM).

The reference electrode records itself a combination of electrophysiological sources (brain and artifacts), so this activity will be present in all other electrodes. A common way of solving this problem, used in all localization approaches, is to construct an average montage (ARM) by subtracting from all CRM recorded signals an "average reference signal" (i.e. the mean of all CRM measures).

Still, the ARM has an important drawback from a BSS point of view: the measures are no longer linearly independent, so the separation solution is degraded. Therefore, we propose in this paper to evaluate the influence of the augmented average montage (AARM) introduced in [9] and of the resulting BSS solution (used for artifact elimination) on the localization. A second objective is to propose a new reliable simple method for the ECD localization of the rhythmic ictal activity, based on the moving dipoles approach. To validate this study, we compared the anatomical concordance between ictal source localizations with the epileptogenic zone defined using depth electrodes.

II. EEG montage selection

According with the physics nature of the electric potentials, they are determined up to an arbitrary constant (a reference potential) [10], this leads us to the model for EEG recordings:

$$\mathbf{x}_{sp} = \mathbf{A}\mathbf{s} + \mathbf{1}_m \mathrm{r} + \mathbf{n} \qquad (1)$$

This study was supported by the French Ministry of Health (PHRC 17-05, 2009) and by the Ligue Française Contre l'Epilepsie.

C. Person, V. Louis-Dorr and D. Wolf are with Centre de Recherche en Automatique de Nancy (CRAN, UMR 7039), Nancy-Université, CNRS, France (christophe.person@ensem.inpl-nancy.fr, valerie.louis@ensem.inpl-nancy.fr, didier.wolf@ensem.inpl-nancy.fr).

L. Koessler and L. Maillard are with Centre de Recherche en Automatique de Nancy (CRAN, UMR 7039), Nancy-Université, CNRS and Centre Hospitalier Universitaire de Nancy, Service de Neurologie (l.koessler@chu-nancy.fr, l.maillard@chu-nancy.fr).

P.Y. Marie is with Centre Hospitalier Universitaire de Nancy, Service de Médecine Nucléaire (py.marie@chu-nancy.fr).

with $\mathbf{x}_{sp}$ being the scalp potentials for m channels, $\mathbf{A}$ a propagation (mixing) matrix $(m \times n)$, $\mathbf{s}$ the electrophysiological sources n, $\mathbf{1}_m = [\mathbf{1} \quad \cdots \quad \mathbf{1}]^t$ a $(m \times 1)$ vector of ones, "r" the reference signal and $\mathbf{n}$ a vector m of additive measurement noise. However, in realistic setups (scalp reference electrode), the "r" signal is itself a noisy mixture of sources $\mathbf{s}$ and thus equation (1) writes more accurately as:

$$\mathbf{x}_{sp} = \mathbf{A}\mathbf{s} + \mathbf{1}_m(\mathbf{a}_{m+1}\mathbf{s} + \mathrm{n}_{m+1}) + \mathbf{n} \qquad (2)$$

with $\mathbf{a}_{m+1}$ a vector of n mixing coefficients and n_{m+1} the noise affecting the reference electrode. One can notice that in this form, the unknown reference disappears and some unknown coefficients $\mathbf{a}_{m+1}$ are added to the mixing $\mathbf{A}$. This writing enlightens the fact that, with this modeling, one only uses the m "measuring" electrodes for any further processing (localization) and completely ignores the scalp potential under the reference.

However, if we want to obtain a scalp map with the best spatial resolution, all electrodes should be used, the unknown "r" included. In order to estimate this reference and to reduce its influence in (1) and (2), one can propose an alternative modeling, as follows. Consider the "ideal" zero-referenced EEG recordings as:

$$\mathbf{x}_0 = \mathbf{A}_0\mathbf{s} + \mathbf{n} \qquad (3)$$

with $\mathbf{x}_0$ being the scalp potentials for $(m+1)$ electrodes (reference electrode included), and $\mathbf{A}_0$ a propagation (mixing) matrix $(m+1 \times n)$. One can easily show that models (2) and (3) are equivalent by considering $\mathbf{x}_0 = [\mathbf{x}_{sp} \quad \mathrm{r}]^t$ and the corresponding $\mathbf{A}_0$ matrix, obtained by padding $\mathbf{A}$ with a supplementary zero row and adding the row vector $\mathbf{a}_{m+1}$ to all the rows of the new matrix.

Now, from equation (3), the CRM measures (the only accessible) can be modeled by subtracting the reference electrode from all scalp potentials. Let $\mathbf{x}_{CRM}$ be the EEG CRM (m channels) obtained using a linear transformation $\mathbf{T}_{CRM}(\mathbf{x}_0) \rightarrow \mathbf{x}_{CRM}$ applied on the $(m+1)$ scalp EEG potentials $\mathbf{x}_0$. Thus we have:

$$\mathbf{x}_{CRM} = \mathbf{T}_{CRM}\mathbf{x}_0 \qquad (4)$$

where $\mathbf{T}_{CRM} = \begin{bmatrix} \mathbf{I} & -\mathbf{1}_m \end{bmatrix}$, $\mathbf{I} \in \Re^{m \times m}$ is the identity matrix and $\mathbf{1}_m$ the $(m \times 1)$ vector of ones defined before.

In classical localization approaches, one uses the well known ARM, obtained by subtracting the average of the m measured channels from each channel (see [9]).

$$\mathbf{x}_{ARM} = \mathbf{x}_{CRM} - \frac{\mathbf{1}^t}{\mathbf{1}^t\mathbf{1}}\mathbf{x}_{CRM} \qquad (5)$$

The new montage proposed in this paper is called AARM and has $(m+1)$ measures (as if we were measuring the activity at each electrode and thus improving the spatial resolution). This montage is the closest possible evaluation of the original potentials $\mathbf{x}_0$ (and thus of the reference potential also) and it can be found by left multiplication with the pseudo-inverse of $\mathbf{T}_{CRM}$, $\mathbf{T}_{CRM}^{+} \in \Re^{(m+1) \times m}$.

$$\mathbf{x}_{AARM} = \hat{\mathbf{x}}_0 = \mathbf{T}_{CRM}^{+}\mathbf{x}_{CRM} \qquad (6)$$

$$\mathbf{T}_{CRM}^{+} = \begin{bmatrix} \mathbf{I} - \dfrac{\mathbf{1}_m\mathbf{1}_m^t}{\mathbf{1}_{m+1}^t\mathbf{1}_{m+1}} & \dfrac{\mathbf{1}_m^t}{\mathbf{1}_{m+1}^t\mathbf{1}_{m+1}} \end{bmatrix}^t \qquad (7)$$

with $\mathbf{1}_{m+1}$ being a $(m+1 \times 1)$ vector of ones.

The new montage obtained by (6) (called further on AARM) have the first m signals very close to the classical ARM (average reference montage) signals and, on the last row, an estimate of this average (the difference consists in the denominator used for averaging, m in ARM and $(m+1)$ in AARM). It has been shown that AARM has the best BSS performances, compared to the other montages [9].

With this arguments in mind, we propose therefore to use further on the AARM (as being the closest estimate of the original potentials) to perform both localization and BSS.

In the Results section of this work, we evaluate the localization results of this montage, compared to classical ARM. It must be noted that the spatial coordinates of the reference electrode must be known in order to implement a localization method based on AARM.

III. BSS PREPROCESSING METHOD

As mentioned before, scalp measures are generally contaminated by artifacts, especially during epileptic seizures. Most of the time these artifacts cannot be eliminated by simple filtering, and one interesting alternative is blind source separation (BSS) [7, 8, 11]. Although the literature in the field is quite extensive, there is no particularly recommended BSS algorithm.

In general, source separation starts from the mixing model from equation (3). The aim of all BSS methods is to estimate the mixing matrix **A** and the sources **s** by maximizing the statistical independence of the estimated sources. Several methods were described in the literature, either based on second order statistics, estimated from the measures (covariance matrices), or on high order statistics (kurtosis, other high order cumulants) (see for example [11] for an extensive presentation of the BSS problem).

In this work we have decided to used the well known second order statistics algorithm SOBI-RO [12], adapted to auto-correlated sources and robust to measurement noise. On the other hand, as shown in [9], the AARM montage leads to better source separation performances, regardless of the algorithm. We have therefore simply applied SOBI-RO to both ARM and AARM to obtain separated sources. The sources were labeled by a trained neurophysiologist as brain sources or artifacts, and artifact free versions of both montages were reconstructed using only brain sources. These clean EEGs were used further on for localization.

IV. Source localization method

A. *MRI and Head modeling*

Three-dimensional MRI was based on a T1-weighted sequence, with a pixel size of 1.25 mm^2 and slice thickness of 1.25 mm. The same anatomic landmarks (nasion, right and left tragi) were identified on the 3D MRI. The realistic head model was based on a boundary element method, which describes the individual surfaces by triangulation, with about 1700−2000 nodes per model. The segmentation process, identification of the three compartments of isoconductivity (intracranial space, skull, and scalp) was performed with ASA software (ANT Software, Enschede, Netherlands). Automatic 3D segmentation was used, the skull being the dilatation (× 4) of the intracranial space. Triangulation of the surfaces was performed automatically and a realistic EEG transfer matrix was calculated. Specific conductivities were attributed to each volume (0.33 Sie/m for intracranial space and scalp, 0.008 Sie/m for skull, conductivity ratio (skull/scalp) = 1/40).

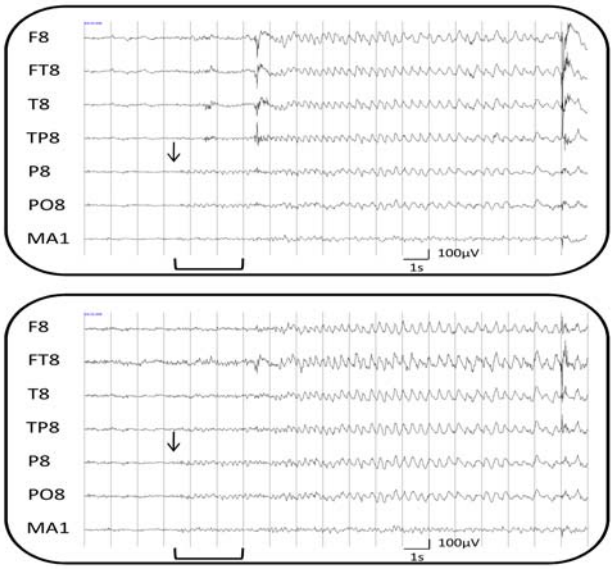

Fig. 1. : Right temporal and reference electrodes of the rhythmic discharge with the AARM (MA1 shows the average reference). Raw EEG is presented in the upper part of the figure and the reconstructed EEG (all sources without physiological artifacts) in the lower part. Seizure onset is indicated by the black arrow and the temporal window of analysis is indicated by the bracket.

B. *Equivalent current dipole*

For source localization analysis, a temporal window was analyzed from the onset of the seizure to 2.5s later. This analysis was performed with a moving dipole approach (i.e. calculation of a new dipole localization, moment and magnitude for each time sample) [13]. To warrant a unique solution, the number of unknown parameters has to be less than or equal to the number of independent measurements (i.e. electrodes). The best location of these limited number of sources is found by computing the surface electric potential map generated by these dipoles using a certain forward model (i.e. how a dipole at a given position and orientation propagates signals to the scalp) and comparing it with the actual measured potential map. This comparison is based on calculating the (average) squared error between the two maps. An automatic initial guess was used to start the dipole fit procedure. Moreover, for consecutive time points of the dipole fit procedure, the fitted position of the previous time point was taken as initial guess for the current time point. All source localizations were performed with ASA software. Unlike in classical approaches for moving dipoles (best fit latency, …), the final estimate of the dipole parameters was made by considering the mean values for all locations, moments and magnitudes during the time window considered for analysis. This option was chosen considering the particular nature of the analyzed signals: ictal rhythms are generally stationary during the analyzed time window, unlike evoked potentials or inter-ictal spikes. In this study, moving dipoles were calculated both with ARM and AARM, for both raw and artifact-free EEG. For each localization we analyzed the goodness of fit (GOF, 1-average square error) and the magnitude of the dipole the during the time window of analysis.

TABLE I

CHARACTERISTICS OF THE MOVING DIPOLE WITH RAW EEG						
	AARM			**ARM**		
	x(mm)	y(mm)	z(mm)	x(mm)	y(mm)	z(mm)
[1]MDP	28.2	-21.4	57.1	23.5	-15.4	47.8
[2]σ	37.5	26.9	26.2	39.6	31.6	28.3
Vol. (cm3)		26.3			33.9	

TABLE II

CHARACTERISTICS OF THE MOVING DIPOLE (RECONSTRUCTED EEG)						
	AARM			**ARM**		
	x(mm)	y(mm)	z(mm)	x(mm)	y(mm)	z(mm)
[1]MDP	25.4	-14.8	57.5	9.7	-6.2	52.2
[2]σ	29.2	33.1	24.5	31.5	34.2	28.9
Vol. (cm3)		23.1			30.8	

[1]MDP: Mean Dipole Position **[2]σ: Standard deviation**

the 10−10 international system (Quickcap; Compumedics Neuroscan, El Paso, TX, USA). The signal was recorded at a 1 KHz sampling rate using a notch filter and digitally filtered between 0.15−200 Hz (SynAmps; Compumedics Neuroscan, Charlotte, NC, USA). The positions of all electrodes and anatomic landmarks (nasion, right and left tragi) were registered with a 3D digitizer system (3Space Fastrak; Polhemus, Colchester, VT, USA).

B. Processed EEG signals

For both ARM and AARM, we analyzed the raw EEG and the reconstructed artifact-free EEG (see figure 1). Source localization was performed on the same temporal window of analysis (duration: 2.567s). For the AARM, the additional signal corresponding to the average was attributed to the reference electrode, placed on the left mastoid (contro-lateral to the epileptic discharge). Identification of artifact sources (after BSS) was done by a trained neurophysiologist.

V. RESULTS AND DISCUSSION

A. Subject and EEG recordings

One drug-resistant partial epilepsy patient (female, 36 years old) with temporal lobe epilepsy was investigated in this study. Patient gave his informed consent and the study was approved by the ethics committee (CPP) of Marseille. Scalp ictal discharge was recorded in the right temporal area. Rhythmic discharge was about 4-5 Hz and had a low (1.5) signal to noise ratio. Because several hypotheses were proposed by the non-invasive investigations, patient underwent stereoelectroencephalography with ten depth electrodes placed in the right temporal lobe. HR-EEG data were recorded using 64 scalp electrodes placed according to

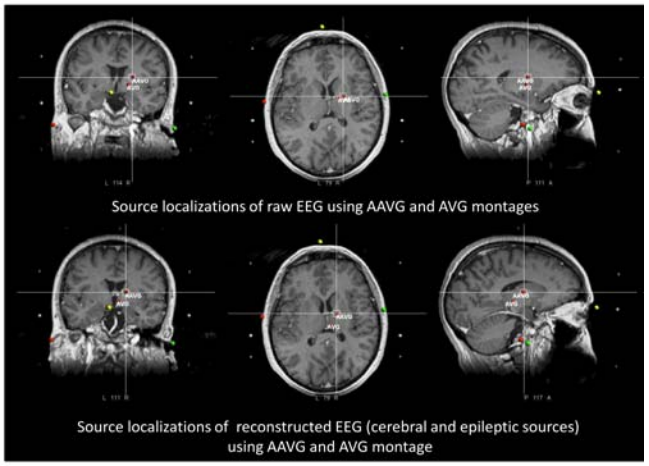

Fig. 2. Mean dipole location during the seizure with raw EEG (top) and reconstructed EEG (bottom). Mean dipole locations with AARM and ARM are co-registered on the individual MRI of the patient.

To compare the results and study the influence of both montage and source separation, we calculated the mean position of the moving dipole, the standard deviation along the three axes and the volume defined by this spatial dispersion. Moreover, in addition to this spatial characterization, we calculated the goodness of fit during the temporal window of analysis and the means and standard deviations of the magnitude of the moving dipole.

According to Table I and II, the standard deviation of the dipole position is better using the AARM than the ARM, and consequently the 3D volumes defined by the displacement of the dipole were also smaller. These results were verified both on raw EEG and reconstructed EEG.

All source localizations are concordant with the epileptogenic zone defined by the depth EEG. These coordinates correspond to the insular cortex which is implicated secondarily during the seizure (see figure 2). In depth, the initial discharge (low amplitude fast discharge) was located in the right anterior and medial temporal lobe and then propagated to the insular region according a rhythmic activity with a frequency equal to this EEG recording (for more details, see [2]). Clinically, mean dipole positions seem to be better using the AARM (more lateral).

Concerning the dipole fit, GOF was consistently better using the AARM and BSS (tables III and IV). Combination of the two methods enhanced the GOF by 2.1%, and mean magnitudes of the dipoles were smaller. This result can be explained by the subtraction of the physiological artifacts, which diminish the global power of the signal and so the magnitude of the dipole. The standard deviation of the magnitudes was smaller in the AARM case, compared to ARM (i.e. the dipole magnitude was more stationary during the temporal window of analysis), probably because physiological artifacts cause local augmentation of magnitude.

VI. CONCLUSION

This study shows that preprocessing combining AARM re-referencing and BSS allows more precise and reliable ictal source localizations than the raw EEG. Unlike for interictal or evoked potentials, it is important to notice that ictal source localization, performed on a long temporal window of analysis, gives an important number of dipole positions. In this case,

we noted that mean dipole position seems to be more appropriate than the best fit latency, especially when raw EEG is used. This can be explained by physiological artifacts, which can induce strong magnitude and a high goodness of fit. We have also shown that preprocessing reduces the displacement of the dipole (smaller volume), permitting thus a more reliable identification of the epileptogenic zone.

Actual results show an epileptogenic zone concordant with the one defined by depth EEG. Other ictal discharges are currently investigated. A complete evaluation of the influence of the presented preprocessing on source localization will be presented in a future work.

REFERENCES

[1] S. Baillet, et al., "Electromagnetic brain mapping", *IEEE Signal Process Mag* , p. 14–30, 2001

[2] L. Koessler et al.,"Source localization of ictal epileptic activity investigated by high resolution EEG and validated by SEEG", *Neuroimage*, 2010

[3] M. Gavaret et al., "Source localization of scalp-EEG interictal spikes in posterior cortex epilepsies investigated by HR-EEG and SEEG", *Epilepsia*, vol. 50, p. 276-89, 2009

[4] L. Maillard et al., "Combined SEEG and source localisation study of temporal lobe schizencephaly and polymicrogyria", *Clin Neurophysiol*, vol. 120(9), p. 1628-1636, 2009

[5] II. Goncharova et al., "EMG contamination of EEG: spectral and topographical characteristics", *Clin Neurophysiol,* vol. 114(9), p. 1580–93, 2003

[6] E. Niedermeyer and F. Lopez Da Silva, "Electroencephalography: basic principles, clinical applications, and related fields." 5th ed. Lippincott, Williams & Wilkins, 2004

[7] TP. Jung et al., "Removing electroencephalographic artifacts by blind source separation", *Psychophysiology,* vol. 37(2), p. 163–78, 2000

[8] N. P. Castellanos, V.A. Makarov, "Recovering EEG brain signals: artifact suppression with wavelet enhanced independent component analysis", *Journal of Neuroscience Methods,* vol. 158, p. 300-312, 2006

[9] R. Salido-Ruiz, R. Ranta, V. Louis-Dorr, "EEG Montage Analysis in Blind Source Separation", 7th IFAC MCBMS conference, 2009, Aalborg, Denmark

[10] R.D. Pascual Marqui, "Discrete, 3D Distributed, linear imaging methods of electric neuronal activity. Part 1: exact, zero error localization", arXiv:0710.3341 [math-ph], 2007-October-17.

[11] A. Cichocki, S. Amari, "Adaptative Blind Signal and Image Processing Learning Algorithms and Applications", John Wiley & Sons, 2002.

[12] A. Belouchrani, A. Cichocki, "Robust whitening procedure in blind source separation context", *Electronics Letters*, vol. 36, no. 24, p. 2050-2053, 2000.

[13] M. Scherg, "Fundamentals of dipole source potential analysis". In: Grandori, F., Hoke, M., Romani, G.L. (Eds.), Auditory Evoked Electric and Magnetic Fields. Karger, Basel, p. 40-69, 1990.

TABLE III

DIPOLE FIT (RAW EEG)		
	AARM	**ARM**
GOF (%)	68.2	67.0
$^{3}M_{AVG}$	321.3	385.8
$^{4}M_{\sigma}$	208.8	270.3

TABLE IV

DIPOLE FIT (RECONSTRUCTED EEG)		
	AARM	**ARM**
GOF (%)	70.3	69.5
$^{3}M_{AVG}$	299.3	304.1
$^{4}M_{\sigma}$	184.5	213.1

$^{3}M_{AVG}$: Mean Magnitude **$^{4}M_{\sigma}$: Standard deviation Magnitude**